

## Observation of intense two-beam positron diffraction and the precise determination of the positron band gap in rare-gas crystals

E. M. Gullikson,\* A. P. Mills, Jr., and E. G. McRae

*AT&T Bell Laboratories, Murray Hill, New Jersey 07974*

(Received 15 October 1987)

We have measured the energy dependence of the elastic specular reflection of positrons from the (111) surfaces of solid rare-gas crystals. For each sample we observe an intense first-order Bragg peak with a profile closely resembling the ideal "top-hat shaped" profile first derived by Darwin. The well-defined width and center of the peak enables us to determine the positron-energy gap and inner potential as a sensitive test of the positron-gas-atom interaction in the solid.

It is well known that a particle should reflect from a periodic solid if an attempt is made to inject it into one of the forbidden energy gaps.<sup>1</sup> Unfortunately, our first-hand experience of this effect is limited to tiny Darwin band gaps (1  $\mu\text{eV}$ ) for x rays<sup>2</sup> and neutrons,<sup>3</sup> not to speak of the rather artificial "band gaps" of optical interference filters. The energy-band gaps of electrons in solids are not directly visible in low-energy electron diffraction (LEED)<sup>4</sup> because the lowest gaps are invariably at negative energies due to the large attraction (inner potential) of electrons to the solid, and the higher gaps are obscured by inelastic effects. We here report that the Bragg reflection of positrons from rare-gas crystals displays with textbook simplicity the lowest energy gap for a particle in a solid. The nearly perfect reflection of positrons over a range of energies, resulting in a specular profile known (because of its shape) as the "Darwin top hat,"<sup>5</sup> allows us to determine the positron band gap and inner potential with a precision that promises to be a significant test of a band calculation that includes one positron.

Before discussing our experiment it is well to recall an analogous one using electrons to study xenon crystals.<sup>6</sup> In most solids the elastic,  $V_e$ , and inelastic,  $V_i$ , scattering potentials of an electron are comparable,  $V_e \approx V_i$ , and LEED intensities can only be understood by a multiple-beam multiple-scattering calculation.<sup>7</sup> Xenon, and presumably the other rare-gas solids as well, represent an unusual case where  $V_i \gg V_e$  so that the LEED intensities become a kinematical series of Bragg peaks.<sup>6</sup> At very low energies an electron or positron in these solids does not have enough energy to cause electronic excitations and we have the opposite extreme,  $V_e \ll V_i$ , where the Bragg peaks exhibit the ideal Darwin top-hat shape with a width equal to the energy gap. Unlike the large electron inner potential  $V_0$ , the  $V_0$  for positrons is invariably quite small and permits a direct observation of this effect. In the low-energy range accessible to positrons the Darwin reflection is easily calculated using the two-beam approximation.<sup>8</sup> The results are dramatic for the rare-gas solids, but similar Bragg peaks for other materials<sup>9,10</sup> are amenable to the same interpretation.

Our experiment was performed on a magnetically guided slow positron beam equipped with an ultrahigh vacuum chamber and cryogenic target stages located inside a 50 K radiation shield. The low base pressure ( $10^{-10}$  Torr) and

low-temperature shields insured that condensed gas surfaces would remain uncontaminated for several hours. A radioactive source, 8-mCi  $^{22}\text{Na}$ , and a solid Ne moderator<sup>11</sup> produced a beam of  $8 \times 10^5$  slow positrons per second. To reduce the energy spread of the positrons they were accelerated to 5 kV and remoderated with a Ni(100) crystal at 77 K. The resulting beam had an intensity of  $10^5 \text{ e}^+ \text{ sec}^{-1}$ , an energy spread of 27 meV full width at half maximum, and a diameter of less than 5 mm. The elastic specular reflection of positrons was measured as described previously.<sup>10</sup>

The substrate for forming the Xe crystals was highly oriented pyrolytic graphite cleaned *in situ* by heating to about 1200 K for 30 sec. The high-purity Xe gas was condensed onto the substrate at  $10^{-5}$  Torr for 2 min. The Kr and Ar were condensed onto an uncleaned graphite substrate on a liquid He cold finger. The Ne was condensed directly onto the cold-finger copper surface. The Kr, Ar, and Ne crystals were annealed at a temperature that caused the pressure in the vacuum chamber to rise to  $10^{-6}$  Torr.

The elastic specular reflection intensity of 0–8 eV positrons from the Xe surface (see Fig. 1) exhibits a nearly rectangular peak having a maximum amplitude of about 0.9 over a 1.0 eV range of positron energy. Similar results, but with a lower maximum reflection intensity, are also shown in Fig. 1 for Kr, Ar, and Ne surfaces. We identify these peaks with the first-order Bragg reflections from the (111) surfaces. In Fig. 2, these are shown together with higher-order Bragg peaks in a plot of intensity versus  $kd/\pi$  for three of the four rare-gas solids. Here  $d$  is the (111) layer spacing, and  $k$  is the magnitude of the positron propagation vector inside the crystal. It has the expression  $k = [2m(E - V_0)]^{1/2}/\hbar$ , where  $V_0$  is the positron inner potential and  $E$  is the kinetic energy of the positron in vacuum just outside the crystal. The layer spacings are assumed equal to those for bulk crystals.<sup>12</sup> The values of  $V_0$  indicated in Figs. 1 and 2 are derived from a fit to the observed positions of the peaks in Fig. 1. The occurrence of peaks at higher integer values of  $kd/\pi$  (Fig. 2) confirms the assignment of the first-order peak, and shows that for each crystal a single value of  $V_0$  applies over the positron-energy range represented.

We interpret the nearly flat-topped Bragg peaks in Fig. 1 by the two-beam dynamical diffraction theory for a per-

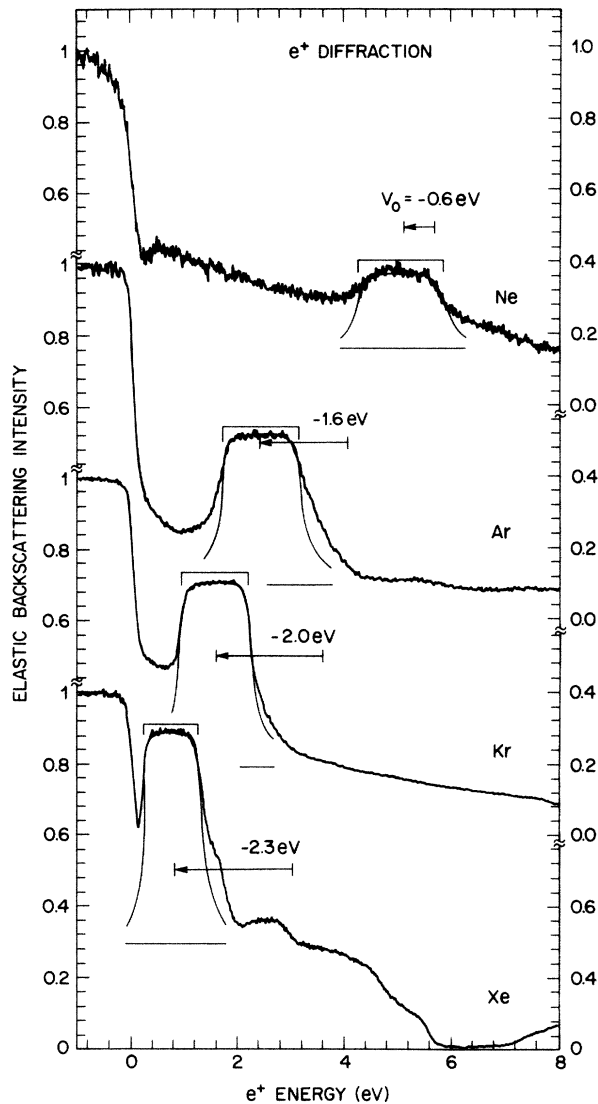


FIG. 1. Positron specular reflection probability vs positron energy,  $E$ , for the (111) surfaces of Ne, Ar, Kr, and Xe.

fect single crystal.<sup>5</sup> According to the theory, in the absence of inelastic scattering of positrons the Bragg peak should exhibit total reflection over a range of energies equal to the band gap corresponding to the momentum transfer. Outside the band gap the reflectivity is represented as falling off sharply, giving the reflectivity curve a "top-hat" shape. We attribute the observed departures from a perfectly flat-topped profile (Fig. 1) to

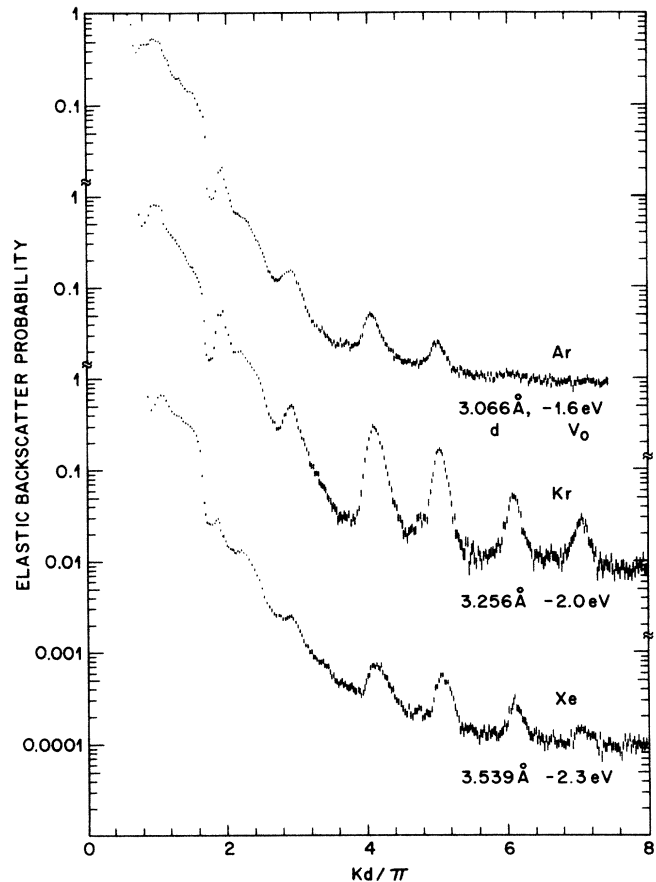


FIG. 2. Positron specular reflection intensity for the same surfaces as in Fig. 1, but plotted vs  $kd/\pi$ , where  $\hbar k$  is the momentum of the positrons in the crystal, and  $d$  is the layer spacing of the planes of atoms parallel to the surface.

inelastic scattering of positrons. The effect of inelastic scattering on diffraction intensities is equivalent to that of "absorption" of particles, and may be represented by adding an imaginary part to the inner potential.<sup>1</sup> Gradually turning on the absorption first causes a rounding of the corners of the top hat, and finally gives it a Lorentzian shape. While the Bragg-peak profiles in Fig. 1 all approach the flat-topped shape characterizing an ideal, nonabsorbing crystal, the observed peak intensities fall short of the total reflection expected for an ideal single crystal. We assume that this is due to amorphous domains making up fractions of the samples ranging from about 10% for Xe (expected to be the best crystal since it

TABLE I. Positronic properties of rare-gas solids.

|    | $d$<br>(Å) | $-V_0$<br>(eV)  | $E_{\text{Bragg}}$<br>(eV) | $E_{\text{gap}}$<br>(eV) | $\text{Im}V_0$<br>(meV) | $\lambda$<br>(Å) |
|----|------------|-----------------|----------------------------|--------------------------|-------------------------|------------------|
| Ne | 2.56       | $0.6 \pm 0.1$   | $5.0 \pm 0.1$              | $1.60 \pm 0.1$           | $10 \pm 3$              | $340 \pm 140$    |
| Ar | 3.066      | $1.55 \pm 0.05$ | $2.45 \pm 0.05$            | $1.50 \pm 0.05$          | $15 \pm 5$              | $230 \pm 90$     |
| Kr | 3.256      | $2.00 \pm 0.05$ | $1.60 \pm 0.05$            | $1.30 \pm 0.05$          | $20 \pm 6$              | $200 \pm 80$     |
| Xe | 3.539      | $2.30 \pm 0.05$ | $0.75 \pm 0.05$            | $1.05 \pm 0.05$          | $60 \pm 20$             | $80 \pm 30$      |

was grown on clean graphite) up to well over 50% in the case of Ne. The theoretical intensity profiles superposed on the experimental ones in Fig. 1 were calculated from the Darwin formula<sup>8</sup> in accordance with the above assumptions. The base of each peak was matched to an estimated background as indicated in Fig. 1, and the height was chosen to fit the data. The values of the band-gap width  $\Delta E_{\text{gap}}$  and imaginary inner potential  $\text{Im}V_0$  were adjusted to fit the data. The derived values of widths  $\Delta E_{\text{gap}}$  and centers  $E_{\text{Bragg}}$  of the band gaps are listed in Table I and are indicated in Fig. 1 by the flat tops that would have been obtained in each case for zero absorption. The effective positron mean-free-path values  $\lambda$  corresponding to the values of imaginary inner potential  $\text{Im}V_0$  used in the fit are also listed (Table I).

The derived values of the mean-free path (Table I) exhibit a decreasing trend in the sense Ne  $\rightarrow$  Xe. This fact, in conjunction with the known decreasing trend of the maximum phonon energies, does not contradict the identification<sup>13</sup> of acoustic-phonon generation as the chief mechanism of inelastic scattering of low-energy positrons in these crystals. The reported value of the inelastic mean-free path in Ar (200 Å, Table I) is the same as determined previously from reflectivity measurements for positrons of slightly higher energy.<sup>13</sup>

The derived values of the energy gaps (Table I) are all about the same, and are an order of magnitude smaller than the simple prediction of twice the (111) Fourier component of the potential deduced from the x-ray scattering form factor.<sup>14</sup> Since the positron-energy gaps are much smaller than the energy for making an exciton, a theoretical model that uses a static potential might be a good starting point for an accurate calculation of the positron band structure. Refinement of the model by including a polarization potential appropriate to the solid would allow us to see how this potential changes from the one that describes free positron-gas-atom scattering.<sup>15</sup>

The applicability of the two-beam dynamical theory, demonstrated in this paper, implies the existence of a standing wave whose nodes sample different positions in the crystal as the energy sweeps through the band gap.<sup>2</sup> In principle, this may be exploited to determine the positions in a crystal of impurity atoms acting as sites of localized absorption. Uniform absorption causes a symmetric rounding of the top-hot intensity profile, but in the case of localized absorption the theory predicts an asymmetric rounding whose sense depends on the atomic arrangement. For example, it should be possible to distinguish between substitutional and interstitial impurity sites. It would be still more interesting, though commensurately difficult, to look for changes in the annihilation angular distribution as the positron energy is varied.

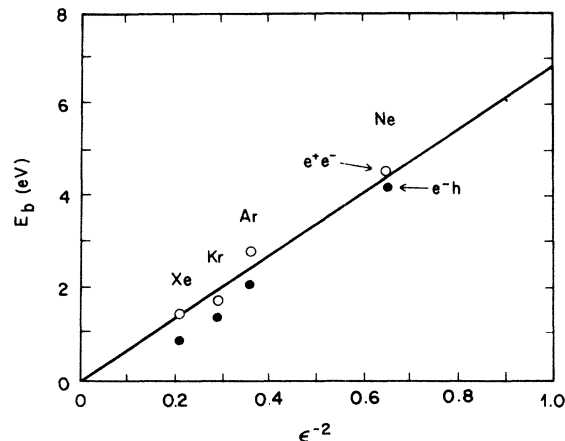


FIG. 3. Positronium and exciton binding energies in the four rare-gas solids plotted vs the inverse square of the low-frequency dielectric constant.

One would suppose that ionic crystals should also exhibit a positron Bragg reflection "top hat," and the first Bragg peak for (100) surfaces of LiF and NaF is indeed very intense and has a slightly flattened top.<sup>10</sup> However, the shape of the peak implies an inelastic potential, 0.15 eV for NaF, that is much larger than would be expected from phonon emission alone. It is possible that large numbers of defects are introduced by the cleaving in vacuum that is used to prepare the samples.

To provide further data to test theories of the positron interaction with the rare-gas solids, we have used our inner potential values from Table I to arrive at precise values for the positronium binding energies  $E_b$  using the method of Ref. 13. In Fig. 3 we plot the four  $E_b$ 's versus the inverse square of the low-frequency dielectric constant. For comparison, the exciton binding energies are also plotted. The data lie remarkably close to the straight line that would hold if the solids were completely homogeneous and the electron and positron effective masses were unity. Considering that the electron and hole masses are not even close to the free-particle mass, the agreement would seem to be fortuitous. On the other hand, the excellent precision of the data would make comparison with a real calculation worth while.

We conclude that an extremely simple dynamic diffraction effect has been seen in positron Bragg reflection from the rare-gas crystals, and that our data can test the positron wave function and band structure predicted by models sensitive to the positron interaction with the condensed atoms.

\*Present address: Lawrence Berkeley Laboratories, Berkeley CA 94720.

<sup>1</sup>J. C. Slater, Phys. Rev. **51**, 840 (1937); J. C. Slater, *Insulators, Semiconductors and Metals: Quantum Theory of Molecules and Solids* (McGraw-Hill, New York, 1967), Vol. 3, Chap. 6.

<sup>2</sup>B. W. Batterman, Phys. Rev. **133**, A759 (1964).

<sup>3</sup>G. E. Bacon, *Neutron Diffraction* (Clarendon, Oxford, 1975), p. 68.

<sup>4</sup>J. B. Pendry, *Low Energy Electron Diffraction* (Academic, New York, 1974), Chap. 3; S. Andersson and B. Kasemo, Solid State Commun. **8**, 961 (1970); E. G. McRae and C. W. Caldwell, Surf. Sci. **57**, 77 (1976); I. H. Khan, J. P.

- Hobson, and R. A. Armstrong, *Phys. Rev.* **129**, 1513 (1963); R. A. Armstrong, *Surf. Sci.* **47**, 666 (1975).
- <sup>5</sup>C. G. Darwin, *Philos. Mag.* **27**, 675 (1914).
- <sup>6</sup>A. Ignatjevs, J. B. Pendry, and T. N. Rhodin, *Phys. Rev. Lett.* **26**, 189 (1971).
- <sup>7</sup>D. F. Lynch and A. E. Smith, *Phys. Status Solidi B* **119**, 355 (1983), and references therein.
- <sup>8</sup>E. G. McRae, *Surf. Sci.* **47**, 167 (1975). This paper contains a simplified derivation and convenient exact expression of Darwin's result (Ref. 5).
- <sup>9</sup>For a review, see A. P. Mills, Jr., in *Positron Solid State Physics*, edited by W. Brandt and A. Dupasquier (North-Holland, Amsterdam, 1983), p. 432; A. P. Mills, Jr. and P. M. Platzman, *Solid State Commun.* **35**, 321 (1980); I. J. Rosenberg, A. H. Weiss, and K. F. Canter, *Phys. Rev. Lett.* **44**, 1139 (1980).
- <sup>10</sup>A. P. Mills, Jr. and W. S. Crane, *Phys. Rev. B* **31**, 3988 (1985).
- <sup>11</sup>A. P. Mills, Jr. and E. M. Gullikson, *Appl. Phys. Lett.* **49**, 1121 (1986).
- <sup>12</sup>P. Kõrpiun and E. Luscher, in *Rare Gas Solids*, edited by M. L. Klein and J. A. Venables (Academic, New York, 1977), Vol. 2, Chap. 12.
- <sup>13</sup>E. M. Gullikson and A. P. Mills, Jr., *Phys. Rev. Lett.* **57**, 376 (1986).
- <sup>14</sup>D. Stroud and H. Ehrenreich, *Phys. Rev.* **171**, 399 (1968).
- <sup>15</sup>H. Massey, *Phys. Today* **29** (No. 3), 42 (1976); T. C. Griffith and G. R. Heyland, *Phys. Rep.* **39**, 169 (1978).